Ultrafast Dynamics of Shock Waves in Polymers and Proteins: The Energy Landscape

Hackjin Kim,* Selezion A. Hambir, and Dana D. Dlott†
School of Chemical Sciences, University of Illinois at Urbana-Champaign, Box 01-6 CLSL, 600 S. Goodwin Avenue, Urbana, Illinois 61801
(Received 8 June 1999)

A 4.5 GPa shock pulse producing a cycle of compression heating (<25 ps) and expansion cooling (~1.5 ns) is used to study fast mechanical dynamics of solid organic polymers and proteins. Coherent Raman spectroscopy of a dye in the sample shows that compression occurs by an instantaneous part followed by a second, ~300 ps, structural relaxation process. After expansion, a mechanically distorted structure is produced which does not relax on the <15 ns time scale. The results are interpreted with an energy landscape model.

PACS numbers: 61.41.+e, 62.50.+p, 78.47.+p, 87.15.He

In this paper we use the nanoshock spectroscopy technique [1] to investigate the microscopic response of organic polymers and proteins, subjected to a cycle of shock compression heating followed by expansion cooling, which produces ultrafast large amplitude structural dynamics. The results are interpreted with an energy landscape model.

The nanoshock [1] is a shock pulse with a duration of about 1 ns. The peak pressure is 4.5(±0.5) GPa. The rise time is <25 ps. The pressure relaxes in a few ns. In a typical organic polymer [e.g., polymethylmethacrylate (PMMA)], shock volume compression is ~20%, the shock velocity is ~4 km/s, and the temperature rise is ~125 K [2,3]. A microscopic understanding of fast large amplitude dynamics of materials helps extend current models beyond linear response, and might be relevant to practical problems such as impact resistance of polymers or biological effects of shock waves generated in pulsed laser surgery or lithotripsy.

Structural relaxation of amorphous materials is usually treated in the context of potential energy landscape theories [4]. Relaxation response functions have been measured for weak external mechanical, acoustic, electrical, thermal, and optical perturbations which result from transitions between local energy minima [4,5]. Shock waves allow us to study fast structural evolution processes in the higher energy regions of the landscape difficult or impossible to access by conventional techniques.

Figure 1 diagrams the energy landscape model for shock waves in amorphous materials. First consider the effects of slow, reversible isothermal compression or expansion [Figs. 1(a) and 1(b)]. This problem has been treated recently in the context of molecular dynamics simulations of glasses [6,7]. With reversible compression, the ambient landscape's total potential energy is increased by an amount equal to the work done on the system. The additional potential energy is distributed among atom pairs in a complicated way which changes the entire topography [6,7], created a new "compressed landscape," whose local minima represent quite different structures from the corresponding ambient landscape. The global minima of compressed landscapes are displaced from the ambient landscapes, because compression favors configurational coordinates which increase the density. Slow reversible compression or expansion is a gradual evolution from the lower energy region of one landscape to another.

Instantaneous shock compression (a limiting case) adds extra kinetic energy to every atom and pushes every pair closer together. There is no time to surmount the barriers which separate adjacent local minima, so conformational coordinates are initially unchanged by fast shock compression. Shock compression may be viewed as a *vertical transition* from the initial landscape to a compressed landscape, as in Fig. 1(c). This view of shock compression of amorphous materials as a vertical transition between landscapes is novel. The vertical transition

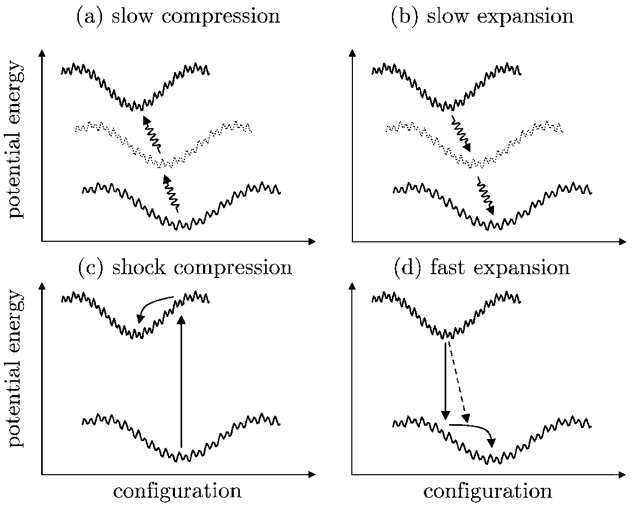

FIG. 1. Energy landscape model. (a), (b) Slow compression and expansion represent a gradual evolution of the landscape. (c), (d) Instantaneous compression and expansion are vertical transitions between ambient and compressed landscapes, followed by a period of structural relaxation. A real expansion is not instantaneous and should be described by the tilted arrow in (d).

 0031-9007/99/83(24)/5034(4)$15.00

between landscapes is reminiscent of and analogous to the Born-Oppenheimer principle for electronic transitions. The fundamental basis for this view is the separation of time scales between vibrational dynamics and structural dynamics.

An instantaneous expansion (another limiting case), as in Fig. 1(d), may similarly be viewed as a vertical transition downward from the compressed landscape to the ambient landscape. Expansion shock fronts cannot be truly instantaneous; otherwise a fast spontaneous entropy decrease would result [8]. Therefore an absolutely vertical downward transition cannot occur. Real shock unloading is better described by the dashed arrow in Fig. 1(d), which tilts toward the global minimum.

In the shock energy landscape model, a cycle of nanoshock compression heating and expansion cooling is understood as follows. After instantaneous shock compression, the system configuration is unfavorable, resulting in structural relaxation over barriers on the compressed landscape toward the lowest states [Fig. 1(c)], to maximize the density. This structural relaxation is analogous to internal conversion which causes the Stokes' shift of fluorescent molecules. A subsequent fast expansion to the ambient landscape will then result in a second structural relaxation, as in Fig. 1(d). The strain energy temporarily stored after the expansion would be maximized by a nanoshock cycle which holds the shock pressure long enough for complete relaxation on the compressed landscape, followed by the fastest possible unloading process.

Experiments were performed on PMMA (average molecular weight 10^6), polyvinyl alcohol (PVA, average molecular weight 1.5×10^5, 99% hydrolyzed), and bovine serum albumin (BSA). The BSA film is a crude model for a dry biological tissue such as skin. The nanoshock technique and the laser apparatus have been discussed previously [1,9,10]. A schematic of the experiment is shown in Fig. 2. A near-IR laser pulse (1.053 μm, 80 ps, 0.3 mJ, 100 μm diameter) ablates a 2 μm thick shock layer which is doped with a near-IR dye, launching a shock through a 5 μm thick PVA buffer layer into a sample layer coated on a glass substrate. The sample is impacted by a tiny ram driven out of the buffer layer at a velocity of $\sim$0.6 km/s. Because of shock reflection from the glass, the sample experiences a two-stage shock [9] to a final pressure of 4.5 GPa. The surface of the ram is curved due to the Gaussian profile of the shock pulse. The probe pulses interrogate a region of $\sim$20 μm in diameter at the center of the $\sim$100 μm diameter nanoshock [9]. In this central region, the pressure and velocity at the nanoshock front remain constant for several nanoseconds [1,9,10], showing we are observing compression by an approximately planar shock front.

The time resolution is approximately the shock round-trip time through the sample [1]. For 0.1 to 0.2 μm thick samples, the time resolution is 50–100 ps. To probe such a thin layer, a sensitive technique has been

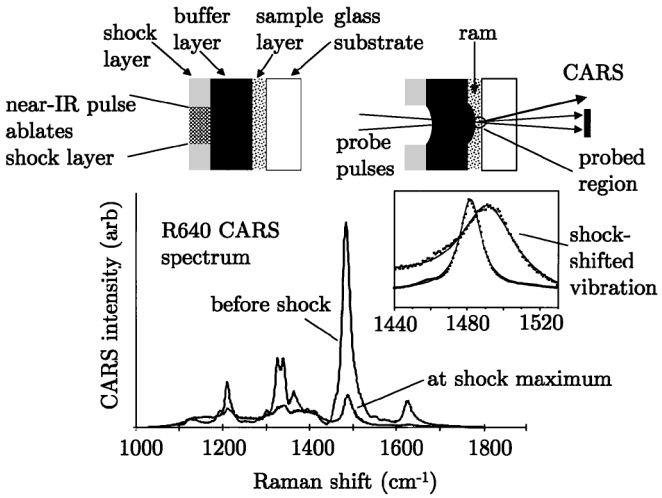

FIG. 2. Top: Schematic of experiment. Ablation induced by a near-IR pulse drives a tiny ram into the sample. Subsequent mechanical dynamics are probed by resonance CARS spectroscopy. Bottom: Resonance CARS spectrum of R640 dye in PMMA. Inset: The most intense vibrational transition is fit by a Lorentzian function (solid curve).

developed using resonance coherent anti-Stokes Raman spectroscopy (CARS) of a dye in the sample. After shock layer ablation $\sim$1.2 ns after the near-IR pulse, broadband multiplex CARS spectra are obtained [10]. One pulse at $\sim$595 nm has a narrow spectral bandwidth ($\sim$1.5 cm^{-1}) which determines the spectral resolution. The second pulse (640–660 nm) has a broad bandwidth ($\sim$350 cm^{-1} FWHM), which determines the width of the probed spectral region. Each spectrum is the result of signal averaging $\sim$8000 laser shots. While signal averaging, the sample is translated on a motorized positioner so every laser shot hits a fresh target.

Recipes for most of the layers have been published previously [1]. The PMMA samples were prepared by spin coating a ketone solution of PMMA with rhodamine 640 (R640). The PVA samples were prepared from aqueous solution with water-soluble sulforhodamine 640 (sR640), which is similar to R640. The BSA samples were prepared by spinning at 600 rpm for 25 s a solution of 300 mg of BSA (Sigma) and 6 mg of sR640 in 5 ml of phosphate buffer ($pH \sim 7$). A polycrystalline sample of pure sR640 was prepared by spraying an aerosol solution of sR640 in methanol:dichloromethane on the glass substrate. Sample thicknesses were measured with a Dektak profilometer. The polymer samples were smooth and 0.1–0.2 μm thick. The protein sample was $\sim$0.3 μm thick and irregular. The dye crystal layer was $<$0.1 μm thick and irregular.

Representative CARS spectra are shown in Fig. 2. When the shock arrives, the dye's electronic transitions are pressure tuned away from resonance, and the CARS intensity drops suddenly. The shock shifts and broadens the dye's vibrational transitions. The most intense transition

at $\sim$1480 cm^{-1} is used as a probe of local structural dynamics, in the same way that time-dependent dye spectra are used to probe structural evolution in polymers and glasses [11], or solvation dynamics of liquids and glasses [12,13]. A computer program fits the $\sim$1480 cm^{-1} transition to a Lorentzian line shape function. Typical fits are shown in the Fig. 2 inset. Because the line shapes consist of $\sim$50 points spaced at 0.8 cm^{-1} intervals, peak shifts of $\sim$1 cm^{-1} can be accurately determined.

Figure 3 shows results for PMMA with a 4.5 GPa shock. The shock front arrives at the PMMA at about 1.2 ns, relative to the arrival of the near-IR pulse at the target. A sudden drop in CARS intensity [Fig. 3(a)], a sudden vibrational blueshift due to the density increase [Fig. 3(b)], and a sudden broadening [Fig. 3(c)] are seen. The broadening is attributed to the temperature increase, although a partial contribution from a small transverse pressure gradient in the probed region cannot be ruled out. The intensity, shift, and width recover over the next few ns as the nanoshock unloads. The shift becomes frozen at $\sim$2 cm^{-1} to the red of its original position, and the width returns to its original value. The intensity decrease for $t > 5$ ns is seen in all of our experiments, and is not associated with sample dynamics. It results from laser beam deflection away from the entrance slit, which is visible by eye, apparently caused by compression and expansion of the buffer layer. The frozen $\sim$2 cm^{-1} redshift indicates that the nanoshock produced a long-lasting (>20 ns) change in the local structure near the dye. The return of the width to its original value indicates that the nanoshock did not produce a broad spread of structural environments.

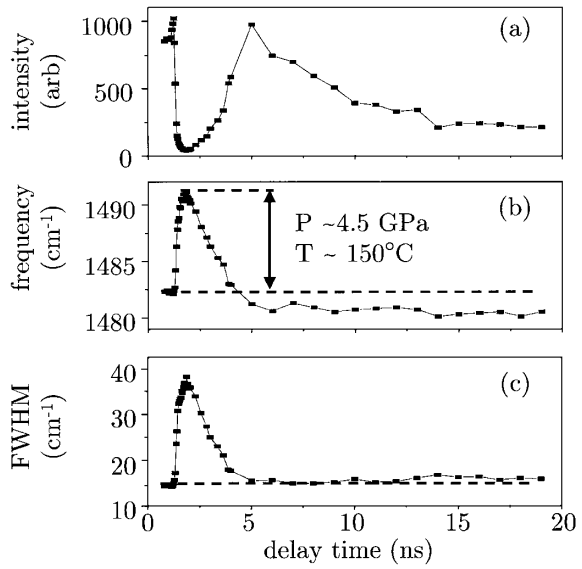

FIG. 3. Data for the $\sim$1480 cm^{-1} R640 vibrational transition in PMMA with a 4.5 GPa nanoshock. (a) CARS intensity. The intensity change for $t > 5$ ns is due to shock-induced beam deflection in the buffer layer. (b) Frequency shift. (c) Linewidth.

In our experiments, the dye responds to a sudden change in the local density of the surrounding solid. To characterize the spectral relaxation, a response function $C(t)$ is defined, suggested by Berg's work on nonpolar solvation in supercooled liquids [12],

$$C(t - t_{\mathrm{arr}}) = \frac{q(t - t_{\mathrm{arr}}) - q_{\mathrm{pk}}}{|q(0) - q_{\mathrm{pk}}|}, \qquad (1)$$

where q may represent either the CARS intensity or the vibrational frequency, t_{arr} is the arrival time of the shock front at the entry face of the sample, $q(0)$ is the value of q before the shock arrives, and q_{pk} is the value of q at the time of maximum shock loading. The intensity response function $C(t)$ for a thin layer of polycrystalline sR640 dye is shown in Fig. 4(a). The dye crystal shock response is instantaneous; the sharp drop in $C(t)$ [90%–10% drop in 110($\pm$10) ps] is limited solely by the shock round trip in the sample layer. The intensity response function $C(t)$ for dye in PMMA [Fig. 4(a)] has a two-part structure. There is an instantaneous drop as in the dye crystals, followed by a slower decay lasting $\sim$300 ps. This slower decay is never observed in crystals, only in polymers and proteins. Figure 4(b) compares vibrational shift correlation functions for three different samples. We prefer to concentrate on the vibrational shift because it avoids complications involving the simultaneous pressure tuning of four electronic resonances, but we are able to measure only the intensity change for the dye crystals [14]. The faster and

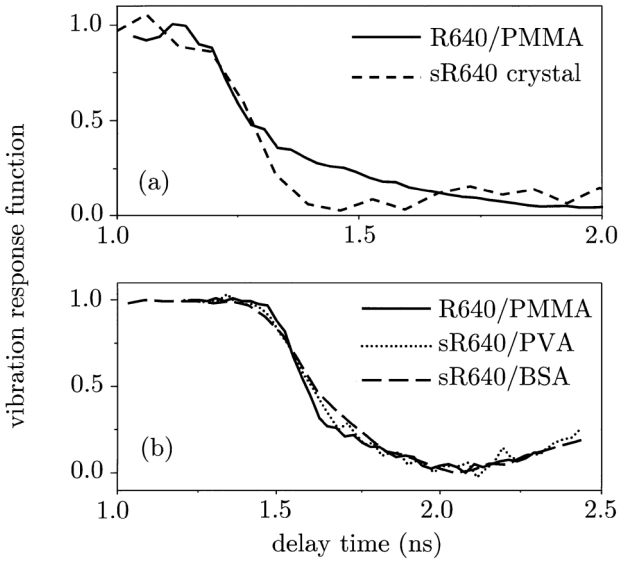

FIG. 4. (a) Intensity response functions for sR640 dye crystals and dye in PMMA. The crystals show an instantaneous response to compression, limited by shock transit time through the sample. In PMMA, there is also a slower part lasting $\sim$300 ps, associated with structural relaxation induced by fast compression. (b) The vibrational frequency response function for PMMA, PVA, and BSA protein. The same structural relaxation process is seen in both polymers and the protein. The response function starts to turn up at $\sim$2.0 ns as the nanoshock starts to unload.

slower parts of the intensity and shift functions have the same time dependence as the intensity data, but the relative amplitudes are slightly different. Figure 4(b) shows an essentially identical two-part shock response is observed for PMMA, PVA, and the BSA protein. The slower decay is a frequency shift of $\sim 5\ \mathrm{cm}^{-1}$, and it can be fit in all cases to an exponential with a 150 ps time constant. The details of the fitting, which convolves the exponential with the 110 ps instantaneous part will be discussed later [14]. The exponential does not preclude the possibility of a nonexponential decay, since we measure the decay only over a narrow time window. After ~ 2.0 ns, $C(t)$ turns back up as the nanoshock starts to decay [Figs. 3(b) and 4(b)].

Two other features of the response function in amorphous solids should be mentioned. The fast part becomes systematically slower as the sample thickness is increased, proving it is limited by the shock transit time. The ~ 300 ps time scale process becomes systematically slower as the shock pressure is decreased from ~ 5 to ~ 2.5 GPa. These results will be discussed more subsequently [14].

The dye frequency blueshift is roughly proportional to the local density increase [15], which ought to be roughly proportional to the distance from the global minimum. After instantaneous shock compression, we see fast structural relaxation on the compressed landscape lasting ~ 300 ps. A dye frequency blueshift of $\sim 5\ \mathrm{cm}^{-1}$ is associated with this relaxation. A 4.5 GPa shock produces an ultimate density increase of $\sim 20\%$ in PMMA, and the corresponding dye frequency blueshift is $\sim 10\ \mathrm{cm}^{-1}$ [Fig. 3(b)]. Thus there is a great deal of fast structural relaxation on the compressed landscape, involving a total local density increase of $\sim 10\%$. If the fast *expansion* caused by nanoshock unloading were instantaneous, the model in Fig. 1(d) shows a vertical transition to the ambient landscape would produce in that case a dye vibrational frequency $\sim 5\ \mathrm{cm}^{-1}$ to the red of the original frequency, i.e., a $5\ \mathrm{cm}^{-1}$ redshift. The experimental value is a $2\ \mathrm{cm}^{-1}$ redshift [Fig. 3(b)]. Evidently some structural relaxation must occur during unloading, so that the unloading path follows the tilted arrow in Fig. 1(d). However, no subsequent structural relaxation occurs on the ambient landscape, at least the 15 ns time scale, The rate of going over barriers on a landscape is $A(\eta)\exp(-\Delta E/kT)$, where ΔE is the barrier height, and $A(\eta)$ is a preexponential factor that depends on the shear viscosity η [5]. Slow structural relaxation on the ambient landscape is understood as arising from the very large viscosity of PMMA below the glass-transition temperature of $\sim 100\,^{\circ}\mathrm{C}$. The very fast structural relaxation seen on the compressed landscape suggests a shock-induced shear viscosity decrease of many orders of magnitude. This very great viscosity drop under shock conditions is consistent with the very few existing determinations of shock viscosities [16].

We have observed fast structural relaxation in two solid organic polymers and one solid biopolymer, induced by ultrafast shock wave compression. An energy landscape model is introduced, which describes shock compression as a vertical transition between an ambient and a compressed landscape. The model explains the fast relaxation seen after compression, and shows how a nanoshock cycle can create amorphous solids which are temporarily stuck in local minima high up the ambient landscape, representing kinetically frozen states at ambient pressure with large amplitude mechanical distortions.

This paper is based upon work supported by the National Science Foundation under Contract No. DMR 9714843 and the Medical Free-electron Laser Program. Additional acknowledgment is given to Air Force Office of Scientific Research Contract No. F49620-97-1-0056. Thickness measurements were carried out in the Center for Microanalysis of Materials, supported by the U.S. Department of Energy under Grant No. DEFG02-91-ER45439.

*Present address: Department of Chemistry, Chungnam National University, 220 Kung Dong, Yusung Gu, Taejon, 305-764, Korea.

†Author to whom correspondence should be addressed. Phone: 217-333-3574. FAX: 217-244-3186. Electronic address: dlott@scs.uiuc.edu

[1] G. Tas *et al.*, J. Appl. Phys. **82**, 1080 (1997).
[2] S. P. Marsh, *LASL Shock Hugoniot Data* (University of California at Berkeley, Berkeley, CA, 1980).
[3] I.-Y. S. Lee, J. R. Hill, and D. D. Dlott, J. Appl. Phys. **75**, 4975 (1994).
[4] F. H. Stillinger, Science **267**, 1935 (1995).
[5] H. F. Mark *et al.*, *Encyclopedia of Polymer Science and Engineering* (Rapra Technology, Ltd., Shawbury, Shrewsbury, Shropshire, United Kingdom, 1985–1990), 2nd ed.
[6] D. J. Lacks, Phys. Rev. Lett. **80**, 5383 (1998).
[7] D. L. Malandro and D. J. Lacks, J. Chem. Phys. **107**, 5804 (1997).
[8] Y. B. Zel'dovich and Y. P. Raiser, *Physics of Shock Waves and High-temperature Hydrodynamic Phenomena* (Academic Press, New York, 1966).
[9] S. A. Hambir *et al.*, J. Appl. Phys. **81**, 2157 (1997).
[10] D. D. Dlott, S. Hambir, and J. Franken, J. Phys. Chem. **102**, 2121 (1998).
[11] L. R. Narasimhan *et al.*, Chem. Rev. **90**, 439 (1990).
[12] M. Berg, Chem. Phys. Lett. **228**, 317 (1994).
[13] R. M. Stratt and M. Maroncelli, J. Phys. Chem. **100**, 12 981 (1996).
[14] H. Kim, S. A. Hambir, and D. D. Dlott (unpublished).
[15] I.-Y. S. Lee *et al.*, J. Chem. Phys. **103**, 8313 (1995).
[16] F. E. Prieto and C. Renero, J. Appl. Phys. **44**, 4013 (1973).